

## 20. *On the Coda Waves of Earthquake Motions. (Part 5)*

By Syun'itiro OMOTE,

Earthquake Research Institute.

(Read Oct. 10, 1946 and Feb. 19, 1947.—Received Sept. 20, 1950.)

Chapter 6. Analysis of the Period of Coda Oscillations  
by Takahasi-Husimi's Method.<sup>1)</sup>

### § 21. Takahasi-Husimi's Method of Analysis.

Takahasi-Husimi's<sup>2)</sup> method of analysis aims at finding the two characteristic constants of a vibrating system,  $p$  and  $\epsilon$ , namely, the coefficient of damping and the circular frequency, from a curve recorded by the motion of the vibrating system when it is exposed to irregular external forces. This new method of analysis devised by K. Takahasi will be made use of in our study here, since it seems to be highly fitted for our present purpose of analysing the coda oscillations of earthquake motions.

In our present study, however, the external forces mean the energies that are conveyed as seismic waves. These seismic waves have to be reflected and refracted many times when they reach the surface of the earth or as they pass through some discontinuities within the earth. Therefore it is not to be denied that the seismic waves are likely to have the character of irregular impulsive waves when they are observed by seismometers installed on the earth's surface. But at the same time it is to be expected that regular periodic waves also are to be detected in the records on the same seismometers. It is our aim, therefore, to expand Takahasi's method to cover the case where the external force consists not only of irregular impulses but also of regular periodic waves, and to see what results are derived from the analysis of the records made by the vibrating system in such a case.

---

1) S. OMOTE, *Bull. Earthq. Res. Inst.*, 21 (1943), 458. 22 (1944), 140. 23 (1945), 47. 28 (1950), 49.

2) K. TAKAHASI and K. HUSIMI, *Geophys. Mag.*, 9 (1935), 29.

§ 22. The Expansion of Takahasi's Method.

When the external force that affects the vibrating system is supposedly made up of a regular and an irregular part, the equation of motion of the vibrating system, according to usual notations, will be given by

$$\frac{d^2x}{dt^2} + 2\epsilon \frac{dx}{dt} + n^2x = f(t) \dots\dots\dots(22.1)$$

where  $f(t)$  is an external force. Whence can be set up the equation

$$f(t) = \varphi(t) + Le^{-\epsilon t} \sin pt \dots\dots\dots(22.2)$$

in which  $\varphi(t)$  is the term representing the wholly irregular motions, and the second term represents the periodic motions of a simple harmonic type with damping.

In the case when  $n > \epsilon$ , the solution of the equation (22.1) is given by

$$x = c_1 e^{-\epsilon t} \cos \sigma t + c_2 e^{-\epsilon t} \sin \sigma t - \frac{e^{-\epsilon t} \cos \sigma t}{\sigma} \int f(t) e^{\epsilon t} \sin \sigma t dt + \frac{e^{-\epsilon t} \sin \sigma t}{\sigma} \int f(t) e^{\epsilon t} \cos \sigma t dt \dots\dots\dots(22.3)$$

$$\sigma = \sqrt{n^2 - \epsilon^2} \dots\dots\dots(22.4)$$

That this  $\varphi(t)$  is a wholly irregular disturbance, according to Takahasi's assumption, is to be interpreted to mean

- (1) That  $\varphi(t)$  is not related either with  $x$  or  $dx/dt$ .
- (2) That the mean value of  $\varphi(t)$  is zero.
- (3) That  $\int_{t_1}^{t_2} \varphi(t) dt$  has nothing to do with  $\int_{t_1'}^{t_2'} \varphi(t) dt$  so long as  $(t_1, t_2)$  and  $(t_1', t_2')$  do not have a common domain.

Now, if we put

$$\varphi(t) = \varphi_0(t - \delta_0) + \varphi_1(t - \delta_1) + \dots + \varphi_n(t - \delta_n) + \dots \dots\dots(22.5)$$

where

$$\left. \begin{aligned} t - \delta_i < 0, & \quad \varphi_i(t - \delta_i) = 0 \\ 0 < t - \delta_i < +\Delta t_i, & \quad \varphi_i(t - \delta_i) \neq 0 \\ t - \delta_i > +\Delta t_i, & \quad \varphi_i(t - \delta_i) = 0 \end{aligned} \right\} \dots\dots\dots(22.6)$$

$$\left. \begin{aligned} \delta_{i-1} < \delta_i \\ i = 0, 1, 2, \dots \end{aligned} \right\} \dots\dots\dots(22.7)$$

then, in such a case, the aspect in which one after another of the free oscillations of a vibrating system is stimulated will be shown in the form

$$\begin{aligned}
 x = & \sum [e^{-\varepsilon(t-d_i)} \{c_{1i} \cos \sigma(t-d_i) + c_{2i} \sin \sigma(t-d_i)\}] \\
 & + \frac{Le^{-\alpha t}}{\sqrt{(\alpha^2 - 2\alpha\varepsilon + n^2 - p^2) + 4p^2(\alpha - \varepsilon)^2}} \sin p(t - \tau) \\
 & - \frac{e^{-\varepsilon t} \cos \sigma t}{\sigma} \int \varphi(t) e^{\varepsilon t} \sin \sigma t dt + \frac{e^{-\varepsilon t} \sin \sigma t}{\sigma} \int \varphi(t) e^{\varepsilon t} \cos \sigma t dt.
 \end{aligned}
 \tag{22.8}$$

With respect to the equation (22.8), if we pick up from among the values of  $x$  observed at certain intervals of time those whose deviation from the mean value of  $x$  is positive, and arrange in vertical column the portions of the curve beginning with  $t_s$  where  $x$  is positive, in order to work out the mean of these partial curves, what sort of a curve is to be obtained, provided that we have had a great many such  $x_s$ ?

To make the matter simple, we will divide the motion of  $x$  into two parts,  $x'$ ,  $x''$ , and put

$$x = x' + x'' \tag{22.9}$$

where  $x'$  represents a part that oscillates simply harmonically and  $x''$  the part that oscillates irregularly.

To begin with, let us consider the  $x'$  parts only. If we assume that the sole irregular external force  $\varphi_0$  worked on the vibrating system, the motion of  $x'$  under the influence of this force, to be given by  $x'_0$ , will have the form

$$\begin{aligned}
 x'_0 = & e^{-\varepsilon t} \{c_1 \cos \sigma t + c_2 \sin \sigma t\} \\
 & + \frac{Le^{-\alpha t}}{\sqrt{(\alpha^2 - 2\alpha\varepsilon + n^2 - p^2) + 4p^2(\alpha - \varepsilon)^2}} \sin p(t - \tau) \dots \tag{22.10}
 \end{aligned}$$

(where  $\delta_0$  is treated as zero).

The equation (22.10) can be rearranged into a simpler form. In the following form the phase difference between the first and second terms of the right-hand side of the equation (22.10) is represented by  $A$ , since it can be given any quite arbitrary values:—

$$x'_0 = ae^{-\varepsilon t} \sin \sigma t + be^{-\alpha t} \sin\{p(t - \tau) + A\}. \tag{22.11}$$

Now we will make  $x'_0(t_0) \dots x'_0(t_n)$  represent the various values which  $x'_0$  has at regular intervals of time, or at  $t_0=0, t_1=k, t_2=t_1+k, \dots$  (22.12), ( $k$  being a certain unit of time), and assume that  $\varepsilon$  and  $\alpha$  of  $x'_0$  are equal and so small that the oscillations will last a sufficiently long time. We will further assume that at a certain definite hour,  $t_s$  in (22.12), the first term of the right-hand side of the equation (22.11) had a certain positive value  $h$ . In

such a case, the second term must be greater than  $(-h)$  to make  $x'_0(t_s) > 0$ . If we make  $a$  equal to  $b$ , the above conditions will be satisfied by

$$\pi + \gamma > p(t_s - \tau) + A$$

or

$$2\pi - \gamma < p(t_s - \tau) + A$$

and from this we see that the probability  $P_+$  that makes  $x'_0(t_s) > 0$  when the first term of the right-hand side in the equation (22.10) is equal to  $+h$ , will be given by

$$P_+ = \frac{1}{2} + \frac{\gamma}{\pi}.$$

In the same way, in the case of  $a \sin \gamma = -h$ , the probability  $P_-$  that makes  $x'_0(t_s) > 0$  will be given by

$$P_- = \frac{1}{2} - \frac{\gamma}{\pi}.$$

Generally speaking, under these assumptions, at any time-point defined by the equation (22.12), when the first term of the right-hand side of (22.10) is positive, the probability that makes  $x'_0 > 0$  is larger than when it is negative. This probability becomes still larger as the absolute value of the first term increases. Now if we make up the summation of

$$\sum \{x'_0(t_s)\} \dots\dots\dots(22.13)$$

with regard to a very long period of time—of the values of  $x_0$  at the  $t_s$  that makes  $x_0(t_s) > 0$ —the terms that are small in their absolute values are likely to be cancelled, since there will occur as many of them in the positive as in the negative, while the terms that are large in their absolute values will remain uncanceled in  $\sum \{x'_0(t_s)\}$  for the lack of their negative values to offset them.

What we have considered above about the first term of the right-hand side of the equation (22.10) is also perfectly applicable to the second term of the same equation. With respect to the second term too, we can easily see that terms with the large positive values are added together in  $\sum \{x'_0(t_s)\}$ .

In general, the maximum amplitudes  $a$  and  $b$  of the first and the second terms are not equal to each other, but even here it will be easily seen that terms with larger positive values are added together.

In the second place, we will consider the case where the free oscillation of the vibrating system is stimulated by one after another of the successive external forces. What modifications will it be necessary to make in the above statement?

Let us make  $x'(t_0), x'(t_1) \dots\dots\dots$  represent the values of  $x'$  of the equation

(22.9) at the time-points  $t_1, t_2, \dots, t_n$ , defined in (22.12), and assume  $x'(t_s) > 0$  at the time-point  $t_s$ . In such a case too, when the free oscillations of that vibrating system are being stimulated in the form  $e^{-\varepsilon(t_s-\delta_i)} \{c_1 \cos \sigma(t_s-\delta_i) + c_2 \sin \delta(t_s-\delta_i)\}$ , it will be easily suspected that the term that has a large amplitude has a high probability to make  $x'(t_s) > 0$ . Similarly, with respect to the oscillations of a simple harmonic type due to an external force that is denoted as  $[Le^{-\alpha t} / \{(\alpha^2 - 2\varepsilon + n^2 - p^2)^2 + 4p^2(\alpha - \varepsilon)^2\}^{\frac{1}{2}}] \sin p(t - \tau)$  the same statement will hold good.

Next, we will compare

$$\sum x'(t_s) \dots\dots\dots(22.14)$$

with

$$\sum x'(t_s + k) \dots\dots\dots(22.15)$$

The former is the summation of all the values of  $x'$  at the time-point  $t_s$  that make  $x'(t_s) > 0$ , and the latter is the summation of all the values of  $x'$  at the time-point of  $(t_s + k)$ , namely, after the lapse of one unit time  $k$  from the respective  $t_s$  used in the former summation. From the definition of (22.14) it is not to be expected that all of the values of  $x'(t_s + k)$  should also be positive and it is reasonable to expect that some of the values of  $x'(t_s + k)$  will be negative. Then, statistically, we shall have to put

$$\sum x'(t_s) > \sum x'(t_s + k).$$

These results will lead us to the following conjecture; if we pick up every positive  $x'(t_s)$  and put the value of  $x'(t_s)$  as  $x_0$ , and also assume that time as the point of commencement, then the curve of the values of  $x$  after  $t_s$  may be drawn. In this manner, we can draw many curves of  $x'_0$  that begin with the different positive values of  $x'_0$ , and finally we can calculate their mean value and draw a mean curve of them all. Such a mean curve will make a damping oscillatory curve with its maximum value at the beginning. The mean curve thus obtained is composed of two independent simple harmonic oscillations not in any way mutually connected either with regard to their periods or with regard to the phases, so that if  $x'$  is at its maximum at the beginning, this means that these two curves also have their maximum values at  $t=0$ . The mean curve will be shown by

$$\bar{x}'_+ = \bar{a}^{(+)} e^{-\varepsilon t} \cos \sigma t + \bar{b}^{(+)} e^{-\alpha t} \cos pt \dots\dots\dots(22.16)$$

where  $\bar{x}'_+$  means the average of all the values of  $x'$  that make  $x' > 0$ , and  $\bar{a}^{(+)}$  and  $\bar{b}^{(+)}$  mean the average amplitudes of the first and the second terms of the equation (22.11) when  $x'$  has the + sign. This, however, does not mean that all the terms of  $\bar{a}^{(+)}$  and  $\bar{b}^{(+)}$  are positive in their signs.

Next, we will consider the amplitude  $x$  which is expressed by  $x=x'+x''$  where  $x'$  is a term due to the simple harmonic motions considered above, and  $x''$  is a term due to irregular external forces. In this expression, even if  $x' > 0$ , it does not necessarily follow that  $x > 0$ . But we can pick up a very large number of positive  $x$  and draw curves that begin each with such a positive  $x$ , and calculate and draw an average curve of them all. In this average curve the positive and negative values of  $x''$  will occur in equal numbers, so that the positive and negative effects of  $x''$  will cancel each other, as a result of which the same conclusions will be derived statistically as we get in the case of the curve  $x'$ .

Therefore, if we denote such an average value by  $\bar{x}_+$ , then,  $\bar{x}_+$  probably has the same nature as  $\bar{x}'_+$  and, similar to the equation (22.16), it will be given by

$$\bar{x}_+ = \bar{A}^{(+)} e^{-\varepsilon t} \cos pt + \bar{B}^{(+)} e^{-\alpha t} \cos pt \dots\dots\dots(22.17)$$

where  $\bar{A}^{(+)}$  and  $\bar{B}^{(+)}$  are both constant terms.

Hitherto, we have solely discussed the cases when the deviation of  $x$  from the average is positive. In precisely the same manner, when the deviation is negative, we can find the average  $\bar{x}_-$  of all the negative values of  $x$ , and the following equation will be derived.

$$\bar{x}_- = \bar{A}^{(-)} e^{-\varepsilon t} \cos \sigma t + \bar{B}^{(-)} e^{-\alpha t} \cos pt \dots\dots\dots(22.18)$$

where  $\bar{A}^{(-)}$  and  $\bar{B}^{(-)}$  are the average of the maximum amplitudes of the first and second terms when the sign of  $x$  is negative.

These irregular external disturbances will imply positive and negative motions occurring with equal frequency, and the simple harmonic motion will be distributed symmetrically from its zero line, so that as a whole the average of a great many values of  $x$ ,  $\bar{x}_+$  will be the same as  $\bar{x}_-$  in their absolute value and have the opposite signs.

As the consequence of this, we have

$$\bar{x}_+ + (-\bar{x}_-) = |\bar{A}| e^{-\varepsilon t} \cos \sigma t + |\bar{B}| e^{-\alpha t} \cos pt \dots\dots(22.19)$$

The first term of the right-hand side of this equation represents the free oscillation of the vibrating system, and the second the damping sine waves due to the external forces.

Now if in some way this curve is analysed into its two component curves, we shall be able to find out the damping constants and the periods of the two oscillatory motions. And thanks to Takahasi's method of analysis, we now have the way to determine from seismographs not only the damping constant and the period of a vibrating system but also the damping constants and the periods of the external forces provided that they contain periodical forces.

Table I. Earthquake and its portion that the Takahasi-Husimi's analysis were resorted to.

A	B	C	D	h	E	A	B	C	D	h	E
				s	m m					s	m m
16-1	16	Siwoyasaki	E-W	1	10- 12	37-4	73	New-Guinea	E-W	2	71- 72
16-2	"	"	"	"	12- 14	37-5	"	"	"	"	72- 73
16-3	"	"	"	"	16- 17	37-6	"	"	"	"	82- 84
19-1	19	Kesenuma	N-S	2	14- 15	37-7	"	"	"	"	93- 95
20-1	20	Koti-Yamato	E-W	1	15- 17	37-8	"	"	"	"	100-102
						37-9	"	"	"	"	102-104
20-2	"	"	N-S	"	11- 13	49- 1	49	Mexico	"	"	69- 71
20-3	"	"	"	"	14- 16	49- 2	"	"	"	"	71- 72
54-1	54	Kagi	"	1	30- 32	49- 3	"	"	"	"	72- 73
34-1	34	Celebes Sea	E-W	2	40- 42	49- 4	"	"	"	"	73- 74
36-1	36	Celebes	"	2	40- 41	49- 5	"	"	"	"	82- 84
36-2	"	"	"	"	41- 42	49- 6	"	"	"	"	84- 85
36-3	"	"	"	"	42- 43	49- 7	"	"	"	"	90- 92
36-4	"	"	"	"	43- 44	49- 8	"	"	"	"	92- 94
36-5	"	"	"	"	50- 51	49- 9	"	"	"	2	99-101
36-6	36	Celebes	E-W	2	51- 52	49-10	"	"	"	"	101-103
36-7	"	"	"	"	60- 62	51- 1	51	Peru	E-W	"	56- 58
36-8	"	"	"	"	62- 64	51- 2	"	"	"	"	58- 60
36-9	"	"	"	"	71- 73	51- 3	"	"	"	2	71- 73
37-1	37	New-Guinea	E-W	2	50- 52	51- 4	"	"	"	"	77- 79
37-2	"	"	"	"	53- 55	51- 5	"	Peru	E-W	2	79- 81.
37-3	"	"	"	"	69- 71	51- 6	"	"	"	"	122-124

(to be continued)

(continued)

A	B	C	D	h	E	A	B	C	D	h	E
				s	m m					s	m m
51- 7	51	Peru	N-S	2	56- 58	52-10	52	Chili	E-W	2	121-122
51- 8	"	"	"	"	58- 59	52-11	"	"	"	"	122-123
51- 9	"	"	"	"	59- 61	52-12	"	"	"	"	138-139
51-10	"	"	"	"	70- 72	52-13	"	"	"	"	139-140
51-11	"	"	"	"	72- 74	52-14	"	"	"	"	140-141
51-12	"	"	"	"	80- 82	52-15	"	"	"	"	62- 63
51-13	"	"	"	"	82- 84	52-16	"	"	"	"	63- 64
51-14	"	Chili	E-W	"	150-151	52-17	"	"	N-S	2	66- 67
51-15	"	"	"	"	151-153	52-18	"	"	"	"	67- 68
52- 1	52	Chili	"	"	66- 68	52-19	"	"	"	"	80- 81
52- 2	"	"	"	"	68- 70	52-20	"	"	"	"	82- 83
52- 3	"	"	"	2	80- 81	52-21	"	"	"	"	83- 84
52- 4	"	"	"	"	81- 83	52-22	"	"	"	"	115-117
52- 5	"	"	"	"	83- 85	52-23	"	"	"	"	117-119
52- 6	"	"	"	"	105-107	52-24	"	"	"	"	130-131
52- 7	"	"	"	"	107-108	52-25	"	"	"	"	131-132
52- 8	"	"	"	"	108-110	52-26	"	"	"	"	132-133
52- 9	"	"	"	"	120-121	52-27	"	"	"	"	133-134

A: Curve No.

B: Earthquake No.

C: Epicenter.

D: Component.

E: Portion in which the analysis was made.

Table II. Numerical values of oscillation curves calculated by means of Takahasi-Husimi's method.

Figures in each heading is curve number in Table I.

	16 1	16-2	16-3	19-1	20-1	20-2	20-3	54-1	34 1
1	+154.2	+132.7	+78.2	+65.6	+183.3	+229.1	+206.0	+158.3	+507.5
2	+102.6	+ 63.5	+52.3	+36.5	+ 70.7	+176.6	+169.8	+124.7	+350.5
3	- 29.1	- 46.4	-10.9	+ 5.9	- 25.6	+ 18.3	+ 48.2	+ 26.7	+101.1
4	-102.2	-117.5	-58.6	-29.7	- 79.9	-114.9	- 65.4	- 91.4	-161.4
5	- 83.4	-122.2	-58.2	-56.5	- 73.1	-135.1	-141.1	-159.9	-335.9
6	- 18.6	- 33.0	-21.1	-45.1	- 47.2	- 50.6	-130.4	-140.2	-367.6
7	+ 34.9	+ 51.6	+29.1	- 0.5	- 21.1	+ 70.0	- 70.6	- 39.9	-256.6
8	+ 68.2	+ 89.7	+52.5	+21.5	- 20.1	+133.3	- 30	+ 85.1	- 63.7
9	+ 67.2	+ 67.9	+46.5	+39.4	- 30.1	+ 99.5	+ 13.3	+161.7	+112.1
10	+ 18.7	- 1.5	+14.8	+22.5	- 29.1	+ 6.1	+ 35.6	+145.7	+234.8
11	- 47.1	- 55.5	-21.0	+ 8.7	+ 8.1	- 87.6	+ 40.8	+ 37.0	+256.8
12	- 69.3	- 73.2	-42.1	-15.2	+ 61.6	-117.6	+ 45.4	- 88.5	+176.0
13	- 43.3	- 35.8	-33.6	-25.6	+ 68.7	- 44.3	+ 6.0	-168.2	+ 47.2
14	- 9.4	+ 31.2	- 4.0	-12.3	+ 36.9	+ 39.1	+ 8.5	-161.5	- 67.3
15	+ 32.9	+ 71.5	+21.4	+ 1.1	- 23.7	+ 61.6	- 77.1	- 67.6	-117.8
16	+ 74.2	+ 61.8	+32.5	+ 6.4	- 68.1	+ 29.1	- 58.0	+ 68.3	-106.8
17	+ 68.9	+ 2.5	+25.6	+10.0	- 84.5	- 38.4	+ 5.9	+162.1	- 50.1
18	+ 4.5	- 54.0	- 4.9	+ 6.3	- 52.6	- 84.1	+ 23.9	+169.3	+ 10.6
19	- 71.4	- 74.1	-19.6	- 2.5	+ 10.7	- 72.5	- 44.1	+ 86.5	+ 32.0
20	- 96.8	- 42.9	-35.6	- 6.0	+ 58.6	- 17.4	+ 45.8	- 39.5	- 12.2

	36-1	36-2	36-3	36-4	36-5	36-6	36-7	36-8	36-9	37-1
1	+618.0	+812.1	+757.1	+359.8	+359.8	+334.7	+182.1	+121.5	+118.2	+122.0
2	+509.4	+553.0	+509.5	+147.7	+229.4	+249.0	+136.7	+ 97.0	+ 66.7	+ 99.4
3	+144.6	+303.0	+141.7	- 37.3	+103.5	+ 36.6	+ 51.8	+ 39.7	+ 4.7	+ 44.3
4	-196.1	-184.9	-204.5	-159.1	- 8.2	-180.3	- 42.0	- 48.9	- 60.5	- 16.6
5	-423.2	-521.5	-324.0	- 94.8	-150.1	-264.5	- 73.8	-107.6	- 83.9	- 61.9
6	-391.2	-711.6	-377.0	-105.1	-142.1	-168.6	- 42.0	-137.1	- 65.0	- 91.6
7	-211.8	-573.4	-265.6	- 45.5	- 74.8	+ 36.8	+ 3.9	-104.8	- 26.2	- 94.8
8	- 8.9	-300.9	- 60.4	+ 90.6	+ 39.3	+213.9	+ 40.6	- 53.9	+ 20.2	- 69.1
9	+ 39.9	+ 54.0	+ 95.5	+107.2	+118.9	+240.7	+ 63.6	+ 9.8	+ 52.3	- 11.7
10	+106.8	+222.9	+177.8	+ 75.5	+ 49.5	+132.2	+ 60.4	+ 76.3	+ 42.6	+ 40.4
11	+122.4	+552.4	+196.6	+ 1.9	+ 10.7	- 33.3	+ 39.0	+130.0	+ 39.0	+ 76.1
12	+136.2	+642.8	+180.7	-118.8	- 56.9	-146.1	- 17.6	+164.8	+ 1.1	+ 70.4
13	+ 17.9	+618.8	+104.3	-145.3	-103.5	-147.4	- 74.0	+150.3	- 43.8	+ 60.5
14	+ 25.4	+272.6	- 60.8	-111.2	- 37.6	- 47.1	- 98.4	+ 87.4	- 55.1	+ 36.3
15	-231.2	- 17.3	-253.8	- 45.8	+ 15.9	+102.0	- 73.5	- 21.5	- 32.9	+ 17.9
16	-173.9	-381.0	-286.5	- 75.2	+ 79.8	+176.4	- 11.4	- 96.0	- 9.8	- 28.7
17	+ 17.7	-574.4	-197.3	- 76.8	+ 92.1	+127.5	+ 46.1	-150.0	+ 11.6	- 47.8
18	+ 71.7	-589.9	- 55.8	- 93.9	+ 35.3	- 6.9	+ 56.9	-134.1	+ 8.0	- 69.5
19	-132.3	-444.9	+ 58.9	- 93.4	- 8.1	-150.8	+ 26.1	-111.8	+ 19.9	- 82.1
20	+137.3	-235.8	+301.6	+ 19.5	- 31.9	-190.2	- 11.2	- 71.1	+ 39.4	- 63.2

(to be continued)

(continued)

	37-2	37-3	37-4	37-5	37-6	37-7	37-8	37-9	49-1	49-2
1	+108.7	+ 95.8	+121.7	+88.7	+82.2	+52.9	+83.7	+77.4	+159.4	+118.0
2	+ 86.8	+ 69.5	+ 88.8	+52.1	+45.3	+39.2	+66.5	+58.0	+127.9	+ 81.4
3	+ 27.1	+ 7.3	+ 5.2	+ 1.5	-15.1	+ 7.4	+28.4	+ 9.7	+ 50.3	+ 24.3
4	- 30.4	- 51.6	- 56.1	-22.2	-52.1	-20.3	-11.4	-25.4	- 38.8	- 22.7
5	- 72.9	- 75.8	- 66.7	-29.6	-42.9	-22.7	-36.2	-43.8	- 85.4	- 54.0
6	- 88.4	- 56.5	- 51.6	-27.4	- 6.4	-14.4	-21.2	-53.7	- 81.1	- 45.3
7	- 64.4	+ 1.4	- 35.2	-12.1	+25.6	- 4.1	+ 8.6	-32.5	- 37.2	- 5.6
8	- 22.6	+ 37.3	+ 10.8	+ 7.9	+39.2	- 4.7	+35.3	+43.0	- 0.8	+ 31.5
9	+ 20.9	+ 63.9	+ 56.4	+13.4	+20.2	+ 5.7	+41.2	+17.4	+ 8.7	+ 49.9
10	+ 48.1	+ 50.4	+ 51.2	+12.7	- 1.5	+18.8	+26.2	+15.1	- 17.6	+ 41.9
11	+ 53.8	- 10.1	+ 9.9	- 8.6	-25.4	+24.6	- 7.1	-10.8	- 38.2	+ 30.1
12	+ 39.9	- 59.6	- 64.6	- 0.7	-41.0	+14.5	-34.2	-37.6	- 30.7	+ 5.9
13	+ 18.6	- 72.1	- 88.5	+13.7	-33.7	- 6.0	-50.2	-37.9	+ 7.0	+ 10.3
14	- 11.5	- 28.7	- 40.6	+45.9	-10.9	-27.9	-35.9	-24.5	+ 48.2	- 16.9
15	- 34.9	+ 34.5	+ 27.5	+45.6	+14.2	-34.1	- 4.1		+ 70.8	- 17.7
16	- 45.2	+ 80.5	+ 59.0	+20.2	+29.2	-25.4	+20.6		+ 49.7	- 8.5
17	- 37.3	+ 84.4	+ 57.4	-26.9	+18.0	- 5.0	+29.0		- 9.6	- 20.2
18	- 20.6	+ 38.4	+ 44.3	-49.3	- 1.3	+10.0	+10.5		- 75.1	- 38.5
19	+ 3.7	- 28.1	+ 12.5	-52.0	-18.1	+ 9.4	-21.4		-104.4	- 42.3
20	+ 34.0	- 77.9	- 32.2	-23.9	-15.9	+ 5.7	-41.4		- 66.7	- 45.3

	49-3	49-4	49-5	49-6	49-7	49-8	49-9	49-10	51-1	51-2
1	+113.0	+346.7	+228.1	+253.4	+241.9	+233.9	+179.6	+127.1	+286.7	+236.6
2	+103.8	+288.0	+179.6	+190.9	+172.4	+176.9	+ 79.2	+ 99.1	+228.7	+196.6
3	+ 77.5	+159.7	+ 61.5	+ 61.2	+ 34.8	+ 62.7	- 33.6	+ 28.8	+108.8	+ 85.6
4	+ 29.8	+ 11.6	- 59.8	- 42.4	- 58.8	- 69.8	-113.3	+ 20.9	- 17.0	- 24.9
5	- 26.0	- 98.6	-119.5	- 83.4	-119.5	-166.4	-129.5	-103.4	- 92.2	-151.9
6	- 50.3	-139.8	- 88.1	- 32.6	-113.3	-161.0	- 80.8	-108.0	-121.8	-168.5
7	- 35.3	-119.1	+ 9.0	+ 46.9	- 39.1	- 57.8	- 37.6	- 63.2	- 56.4	-114.6
8	- 0.5	- 43.9	+132.1	+109.3	+ 46.2	+ 80.9	+ 51.7	+ 7.7	+ 19.7	- 15.5
9	+ 25.0	+ 18.0	+216.2	+ 96.0	+ 78.5	+182.9	+144.0	+ 64.4	+ 74.3	+ 65.2
10	+ 25.5	+ 33.0	+204.2	+ 30.6	+ 42.4	+215.3	+122.9	+ 90.0	+ 77.3	+ 87.3
11	- 2.8	+ 18.2	+ 95.4	- 48.1	- 9.9	+153.6	+ 34.5	+ 70.2	+ 17.5	+ 44.4
12	- 51.3	- 25.7	- 54.6	- 94.8	- 69.5	+ 5.0	- 42.8	+ 18.6	- 83.1	- 24.3
13	- 83.6	- 55.3	- 80.1	- 57.7	- 96.4	-125.4	- 86.0	- 37.0	-175.7	- 61.4
14	- 91.8	- 76.0	-154.1	- 14.8	- 80.0	-164.5	- 64.5	- 76.2	-211.7	-112.5
15	- 60.3	- 87.6	- 66.7	+ 35.8	- 32.1	- 89.1	+ 5.6	- 74.8	-168.1	+ 0.6
16	- 5.9	- 99.8	+ 74.6	+ 58.5	+ 8.3	+ 2.0	+106.1	- 38.9	- 62.2	+107.3
17	+ 25.9	-124.7	+175.4	+ 34.5	+ 19.0	+ 92.5	+203.6	+ 12.2	+ 57.7	+176.3
18	+ 47.8	-127.7	+193.3	+ 13.9	- 52.8	+138.2	+220.8	+ 47.3	+140.9	+169.2
19	+ 52.1	- 98.2	+ 83.3	- 46.9	-103.4	+ 84.7	+142.0	+ 55.1	+153.1	+ 90.4
20	+ 45.3	- 40.9	- 55.4	- 40.4	-101.1	- 15.9	- 23.7	+ 30.6	+ 99.3	- 54.9

(to be continued)

(continued)

	51-3	51-4	51-5	51-6	51-7	51-8	51-9	51-10	51-11	51-12
1	+144.5	+214.9	+200.8	+115.0	+803.4	+749.7	+209.1	+140.9	+73.9	+257.4
2	+ 98.2	+182.9	+137.0	+ 89.0	+593.7	+582.3	+147.7	+106.7	+53.5	+212.3
3	+ 5.6	+ 96.4	+ 19.1	+ 17.4	+282.1	+140.9	+ 9.1	+ 27.6	+ 9.8	+ 79.4
4	- 95.7	- 7.7	- 98.7	- 60.8	- 41.8	-366.5	-147.5	- 62.7	-39.5	- 73.8
5	-134.4	- 90.1	-156.6	-101.9	-368.8	-630.1	-224.2	-122.4	-70.3	-188.1
6	-108.8	-125.0	-131.2	- 89.7	-549.3	-654.0	-201.5	-124.0	-66.9	-233.1
7	- 34.7	-110.9	- 36.0	- 29.2	-479.4	-361.9	- 77.0	- 69.1	-31.6	-177.2
8	+ 57.1	- 42.1	+ 57.9	+ 39.5	-126.6	+ 63.8	+ 92.5	+ 11.9	+15.3	- 46.5
9	+113.5	+ 34.8	+112.5	+ 86.5	+286.2	+409.8	+206.1	+ 73.9	+43.2	+ 95.3
10	+111.1	+ 75.9	+105.9	+ 85.2	+556.8	+550.1	+243.0	+108.1	+58.3	+199.7
11	+ 56.5	+ 73.0	+ 36.5	+ 37.7	+585.7	+457.5	+161.0	+ 80.4	+34.0	+281.5
12	- 23.4	+ 24.4	- 37.2	- 26.5	+383.1	+102.8	+ 2.0	+ 14.0	- 7.2	+167.7
13	- 89.1	- 15.0	- 93.0	- 69.7	- 47.4	-289.3	-148.2	- 52.3	-41.1	+ 35.6
14	- 99.3	- 39.9	-102.0	- 75.0	-447.0	-534.8	-248.9	- 98.7	-61.4	- 94.1
15	- 62.0	- 35.5	- 67.7	- 37.6	-687.6	-551.2	-224.2	- 68.6	-24.4	-184.9
16	+ 0.6	- 2.9	+ 7.4	+ 22.6	-632.6	-241.1	- 97.3	- 12.6	+15.3	-212.2
17	+ 57.2	+ 35.5	+ 60.7	+ 67.2	-259.8	+204.8	+ 75.9	+ 53.9	+51.7	-151.4
18	+ 81.2	+ 65.4	+ 91.8	+ 75.3	+210.5	+535.4	+195.1	+ 94.8	+66.1	- 32.9
19	+ 51.0	+ 81.3	+ 67.3	+ 43.7	+546.3	+596.0	+236.2	+ 92.4	+50.7	+ 84.2
20	- 9.4	+ 71.4	+ 14.3	- 12.3	-662.0	+406.2	+163.9	+ 26.1	- 6.8	+163.5

	51-13	51-14	51-15	52-1	52-2	52-3	52-4	52-5	52-6	52-7
1	+282.6	+78.5	+71.4	+639.2	+512.5	+635.2	+473.2	+440.6	+444.6	+329.6
2	+219.9	+51.4	+50.8	+453.4	+383.1	+564.7	+393.2	+380.2	+280.3	+273.0
3	+ 43.5	+ 5.6	+ 5.0	+134.5	+138.9	+356.2	+171.2	+144.1	+ 20.0	+ 76.0
4	-146.6	-46.2	-36.4	-122.8	-132.3	+ 82.8	- 49.9	- 91.5	-211.4	-130.5
5	-267.5	-76.8	-43.1	-291.8	-373.7	-132.4	-303.9	-248.4	-363.6	-242.9
6	-238.6	-62.4	-52.1	-359.0	-373.0	-245.0	-337.1	-234.3	-364.7	-208.8
7	- 88.0	-14.0	-12.9	-293.1	-323.5	-235.4	-229.2	-122.7	-233.5	- 74.4
8	+ 96.0	+43.8	+40.5	- 51.7	- 74.2	-103.5	- 31.1	+ 2.2	- 70.4	+ 29.4
9	+211.5	+78.4	+59.8	+209.5	+168.7	+ 50.4	+130.4	+ 83.5	+111.2	+ 87.3
10	+197.9	+69.4	+56.1	+237.5	+342.4	+108.6	+174.5	+ 48.8	+227.8	+ 60.2
11	+ 95.8	+18.7	+20.7	+153.9	+416.6	+ 24.4	+ 88.8	- 69.4	+244.6	- 8.6
12	- 32.7	-41.6	-19.9	+ 33.2	+213.0	-171.8	- 48.7	-180.6	+121.7	- 40.7
13	-131.7	-76.5	-53.4	-168.5	- 68.3	-334.3	-122.8	-283.7	+ 60.9	- 32.7
14	-134.7	-68.6	-58.9	-249.5	-303.3	-365.2	-225.0	-272.2	- 2.9	+ 31.9
15	- 80.7	-21.1	-30.3	-147.4	-393.9	-246.1	+ 1.2	- 57.5	- 98.5	+ 75.6
16	+ 83.8	+39.1	+15.6	+ 51.3	-268.3	- 5.3	+214.7	+155.6	-162.5	+ 44.1
17	+168.9	+77.0	+46.2	+162.9	- 44.3	+268.9	+352.7	+374.8	-185.6	- 17.8
18	+142.6	+73.6	+59.7	+168.1	+251.5	+495.2	+338.4	+448.7	-162.5	- 87.7
19	- 5.6	+20.9	+37.0	+114.2	+434.7	+591.6	+180.8	+338.9	- 90.5	-112.5
20	-142.9	-31.7	- 6.0	+ 12.1	+393.3	+507.1	-109.9	+173.4	+ 5.2	- 69.8

(to be continued)

(continued)

	52-8	52-9	52-10	52-11	52-12	52-13	52-14	52-15	52-16	52-17
1	+275.9	+110.2	+107.9	+83.8	+103.4	+127.8	+121.7	+771.2	+896.1	+248.5
2	+202.2	+ 72.5	+ 68.9	+47.7	+ 89.3	+ 92.5	+ 90.9	+525.2	+645.1	+179.7
3	+ 38.7	+ 24.5	+ 31.1	- 4.1	+ 31.5	+ 13.3	+ 23.8	+ 39.0	+111.3	+ 91.2
4	-105.1	- 41.2	- 24	-58.8	- 35.8	- 68.7	- 33.0	-430.3	-462.8	-111.5
5	-184.8	- 72.2	- 45.0	-67.7	- 90.6	-106.7	- 54.3	-702.7	-818.4	-207.5
6	-143.7	- 57.4	- 42.7	-44.2	- 81.7	- 80.1	- 27.9	-650.6	-816.0	-204.8
7	- 41.2	- 13.3	- 22.4	- 9.3	- 37.5	- 12.8	+ 15.2	-282.2	-357.4	-118.7
8	+ 71.9	+ 22.6	+ 11.8	+33.7	+ 20.2	+ 57.9	+ 55.3	+202.4	+181.8	+ 18.3
9	+124.6	+ 31.0	+ 35.6	+44.5	+ 60.8	+100.3	+ 55.8	+596.9	+697.0	+144.0
10	+109.1	+ 21.3	+ 14.9	+34.3	+ 53.2	+ 69.6	+ 12.4	+738.4	+914.6	+206.8
11	+ 47.1	- 14.5	+ 3.2	+ 9.9	+ 21.4	+ 14.4	- 47.2	+561.7	+805.5	+189.2
12	- 43.8	- 21.5	- 17.1	-15.5	- 14.2	- 59.1	- 85.6	+119.1	+205.6	+ 57.8
13	-103.6	- 12.4	- 31.1	-24.3	- 34.3	-112.6	- 91.0	-365.3	-307.6	- 73.1
14	-146.4	+ 0.8	- 11.3	-20.6	- 23.8	-100.9	- 56.1	-691.4	-719.4	-201.6
15	-103.7	+ 16.8	+ 4.8	- 7.9	- 4.5	- 39.8	+ 1.3	-684.6	-798.9	-237.3
16	- 22.8	+ 12.3	+ 23.9	+ 4.0	+ 18.1	+ 48.5	+ 37.4	-383.7	-465.5	-175.4
17	+ 55.6	+ 15.7	+ 27.6	+14.1	+ 28.4	+101.2	+ 38.7	+ 94.7	+ 35.4	- 38.3
18	+119.2	+ 14.2	+ 10.6	+ 5.4	+ 16.1	+101.5	+ 13.3	+503.4	+512.8	+116.8
19	+ 98.4	+ 9.7	- 2.4	- 9.5	- 19.1	+ 46.6	- 18.7	+678.6	+681.2	+183.1
20	+ 41.4	- 11.5	- 9.5	-11.2	- 42.3	- 33.8	- 30.4	+540.1	+563.8	+234.2

	52-18	52-19	52-20	52-21	52-22	52-23	52-24	52-25	52-26	52-27
1	+299.3	+105.6	+107.9	+138.2	+155.3	+184.4	+185.9	+189.3	+111.9	+164.2
2	+248.5	+ 81.9	+ 92.8	+135.4	+116.4	+135.2	+ 89.1	+122.0	+ 52.2	+ 80.3
3	+105.9	+ 27.3	+ 52.6	+ 75.0	+ 40.4	+ 16.6	+ 0.6	- 2.7	+ 14.3	+ 4.3
4	- 63.8	- 34.9	- 4.7	+ 13.0	- 35.4	- 93.6	-113.9	-119.9	- 20.2	- 98.9
5	-189.5	- 82.4	- 61.5	- 40.6	- 94.2	-140.7	-139.7	-167.7	- 45.1	-137.7
6	-230.5	-100.8	- 93.9	- 76.0	- 72.0	-111.4	-102.9	-106.5	+ 14.6	- 92.4
7	-175.7	- 85.4	- 84.7	- 68.0	- 21.0	- 22.9	- 7.6	- 2.0	+ 20.7	- 9.8
8	- 61.8	- 49.4	- 56.4	- 19.2	+ 0.9	+ 64.5	+ 79.5	+120.9	+ 66.9	+ 74.2
9	+ 51.4	- 4.4	- 7.5	- 1.9	+ 25.9	+108.6	+125.4	+165.7	+ 44.8	+138.1
10	+116.9	+ 29.4	+ 38.3	+ 1.3	+ 10.4	+ 83.5	+116.7	+144.5	+ 45.1	+107.4
11	+119.6	+ 40.6	+ 64.1	+ 13.4	- 17.2	+ 20.8	+ 39.9	- 2.4	+ 5.3	+ 61.0
12	+ 72.2	+ 26.8	+ 59.2	- 3.4	- 13.0	- 45.2	- 28.5	- 86.1	- 6.1	- 74.5
13	+ 0.1	- 0.6	+ 19.7	- 46.1	+ 5.2	- 73.6	- 91.4	-171.2	- 4.2	-152.4
14	- 55.7	- 30.1	- 22.4	- 79.1	+ 23.2	- 64.4	-107.1	-122.4	- 20.9	-171.7
15	- 74.9	- 46.6	- 56.9	- 83.9	+ 47.0	- 24.7	- 68.7	- 32.9	+ 21.4	- 95.0
16	- 58.4	- 41.2	- 70.8	- 58.2	+ 31.1	+ 24.4	- 10.4	+ 85.0	- 4.8	- 2.2
17	- 27.2	- 17.0	- 48.7	- 22.2	- 18.2	+ 54.1	+ 86.3	+149.4	+ 38.9	+122.5
18	- 5.9	+ 18.6	- 15.3	- 6.9	- 41.5	+ 44.5	+114.7	+106.8	- 19.5	+151.8
19	- 15.9	+ 50.9	+ 26.1	+ 13.0	- 74.4	+ 16.6	+ 89.8	+ 31.4	+ 9.1	+139.0
20	- 41.4	+ 68.5	+ 58.6	+ 3.1	- 63.6	- 19.0	+ 24.6	- 70.9	- 25.6	+ 53.1

§ 23. **Analysis of the Seismograph.**

The earthquakes and the portions of their coda oscillations analysed by Takahasi's method are tabulated in Table I. The oscillation curves obtained as the result of the analyses are given in Table II and Figs. 1-7. Of these oscillation curves, some have a distinct periodicity which at once convinces us that they are composed of a single sine curve, while others are not so simple and are supposed to be composed of two sine curves of the damping nature.

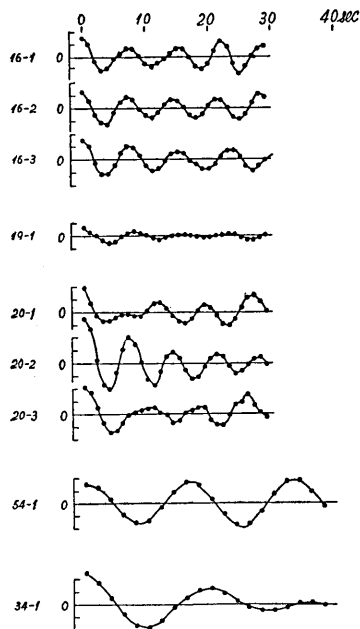


Fig. 1. Oscillation curve.

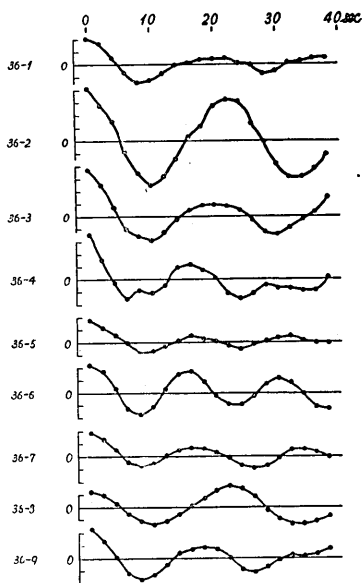


Fig. 2. Oscillation curve (Celebes earthquake).

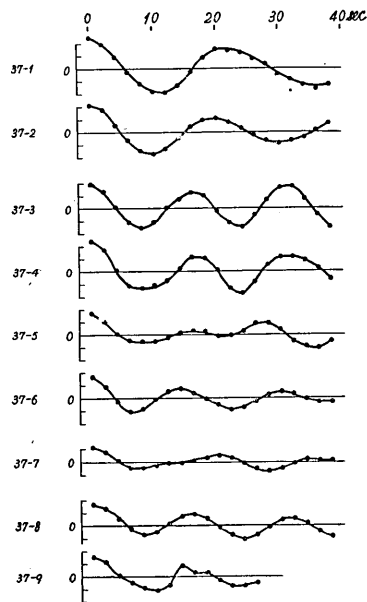


Fig. 3. Oscillation curve (New Guinea earthquake).

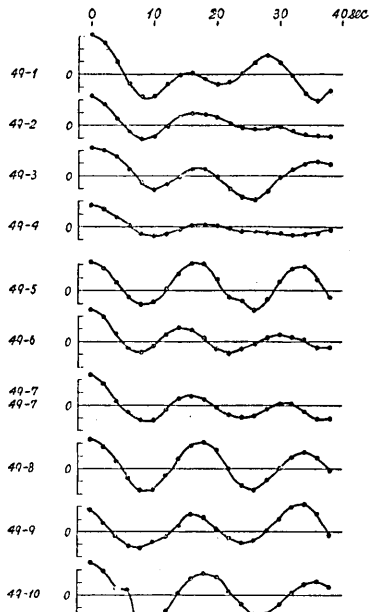


Fig. 4. Oscillation curve (Mexico earthquake).

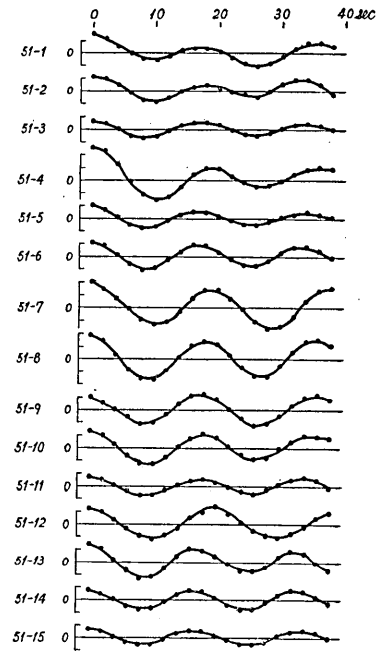


Fig. 5. Oscillation curve (Peru earthquake).

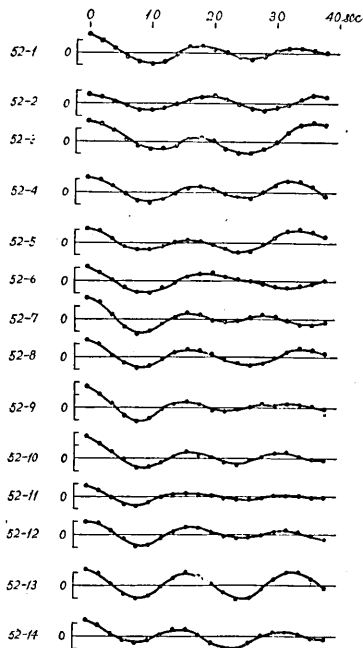


Fig. 6. Oscillation curve (Chili earthquake E-W comp.).

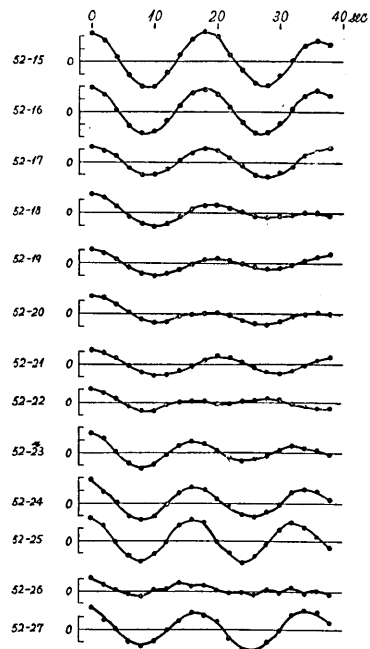


Fig. 7. Oscillation curve (Chili earthquake N-S comp.).

§ 24. **Decomposition of an Oscillation Curve into its Component Curves.**

As most of the oscillation curves obtained by Takahasi's method of analysis are composed of two sine curves of the damping nature, it is necessary to decompose them into their two component curves. If we put the amplitude of the oscillation curve corresponding to the time  $t$  as  $y$ , then  $y$  will be given by

$$y = Ae^{-\alpha t} \sin n(t - \tau_1) + Be^{-\alpha t} \sin p(t - \tau) \dots\dots\dots(24.1)$$

which is written as

$$y = \alpha_1 e^{\beta_1 t} + \alpha_2 e^{\beta_2 t} + \alpha_3 e^{\beta_3 t} + \alpha_4 e^{\beta_4 t} \dots\dots\dots(24.2)$$

where  $\alpha$  and  $\beta$  are complex numbers. As the value of  $y$  is given at certain intervals of time (and these intervals of time are given by  $t_\gamma = t_1 + \gamma h$ ,  $\gamma = 1, 2, \dots$ )  $y_\gamma$  will be written as

$$y_\gamma = \alpha_1 e^{\beta_1(t_1 + \gamma h)} + \alpha_2 e^{\beta_2(t_1 + \gamma h)} + \alpha_3 e^{\beta_3(t_1 + \gamma h)} + \alpha_4 e^{\beta_4(t_1 + \gamma h)} \dots\dots\dots(24.3)$$

Now, putting

$$z_1 = e^{\beta_1 h}, \quad z_2 = e^{\beta_2 h}, \quad z_3 = e^{\beta_3 h}, \quad z_4 = e^{\beta_4 h} \dots\dots\dots(24.4)$$

$z_1, z_2, z_3$  and  $z_4$  are to be obtained as the set of four roots of the fourth order equation

$$z^4 + s_1 z^3 + s_2 z^2 + s_3 z + s_4 = 0, \dots\dots\dots(24.5)$$

provided

$$\left. \begin{aligned} s_1 &= -(z_1 + z_2 + z_3 + z_4) \\ s_2 &= z_1 z_2 + z_2 z_3 + z_3 z_4 + z_4 z_1 \\ s_3 &= (z_1 z_2 z_3 + z_2 z_3 z_4 + z_3 z_4 z_1 + z_4 z_1 z_2) \\ s_4 &= z_1 z_2 z_3 z_4 \end{aligned} \right\}, \dots\dots\dots(24.6)$$

then we shall obtain the values of  $\epsilon, n, \alpha$  and  $p$  from the solution of the observation equations. Then replace them in (24.2) and carry out the calculation of the least square once more, and we shall obtain the remaining four constants  $A, B, \tau_1$  and  $\tau$ . In short, we thus come to know all the coefficients of the two component curves.

Now we are going to analyse the oscillation curves in Figs. 1-7 by means of the above method of analysis, but some of the oscillation curves are so simple that they are supposed to be composed each of a single sine curve of the damping nature. In such a case, the third and the fourth terms of the equation (24.2) are lacking, so that, instead of the equation of the fourth order of (24.5), a quadratic equation

$$z^2 + s_1 z + s_2 = 0 \dots\dots\dots(24.7)$$

will be solved and a set of conjugate complex roots of the equation will be used for the determination of the sine curve.

3) C. RUNGE und H. KÖNIG, "Vorlesungen über Numerischen Rechnen," Berlin (1924), 231.

### § 25. Analysis of Oscillation Curves.

We picked up ten curves out of the Figs. 1-7 which were supposed to be composed of two sine curves, and executed the calculation explained in the last paragraph with the results given in Table III. These calculated curves are compared with the observed ones in Fig. 8, in which I is the oscillation curve obtained by Takahasi's method of analysis, II the calculated curve, III and IV the two component sine curves into which curve I was decomposed. In all the cases in Fig. 8, the observed curves agree fairly well with the calculated ones but some curves in III and IV differ from each other by  $\pi$  in

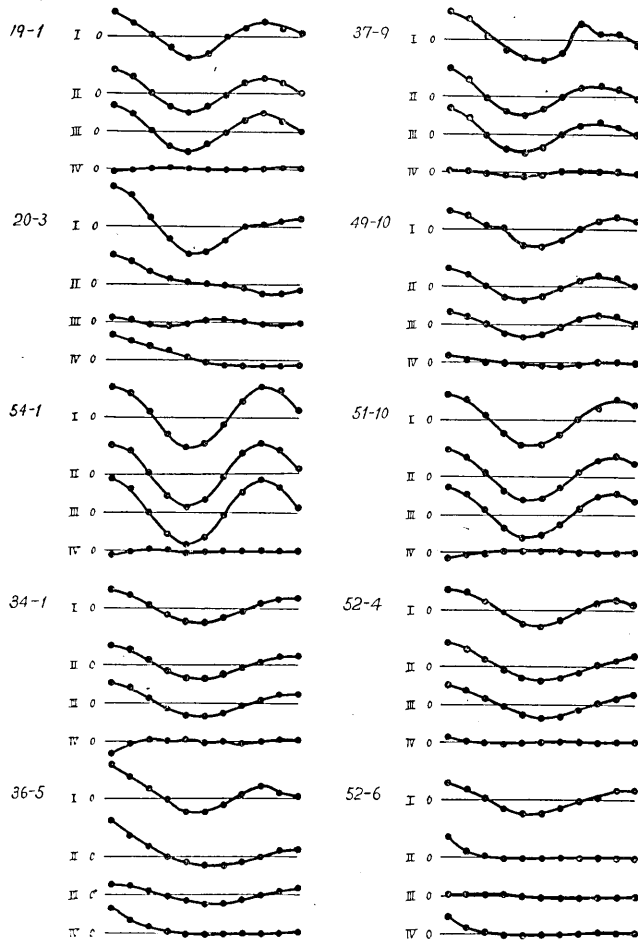


Fig. 8. I; Oscillation curve. III, IV; curves decomposed the curve I into it's elementary two curves. II; III+IV.

their phases, so that some have the negative value at the beginning. Anyhow, with respect to these two component curves, we notice that the curve that has a large damping coefficient affects the curve II only slightly while the curve that has a small damping largely determines the shape of the oscillation curve.

Table III. Constants of damping sine curves obtained by solving the 4<sup>th</sup> equation.

Curve No.	$\epsilon$	$\alpha$	$n$	$p$	$Tn$	$Tp$	$A$	$B$
19- 1	-0.0707	-0.5383	44°45'	56°29'	16.08	6.4	+ 34.51	- 3.77
20- 3	-0.0311	-0.1577	61°41'	19°31'	5.9	36.88	+ 9.79	+ 67.58
54- 1	-0.0115	-0.6712	44°01'	67°33'	16.36	10.66	+ 89.05	- 12.62
34- 1	-0.0899	-0.9502	36°22'	54°46'	19.84	13.14	+282.28	- 31.94
36- 5	-0.0364	-0.5728	33°10'	23°50'	21.70	30.25	+ 54.78	+127.81
37- 9	-0.0942	-0.3935	45°14'	46°55'	15.92	15.46	+ 35 03	+ 4.09
49-10	-0.0145	-0.3234	43°57'	42°25'	16.40	17.00	+ 33.06	+ 18.63
51-10	-0.0348	-0.5204	40°33'	38°14'	17.76	19.00	+ 72.92	- 1.35
52- 4	-0.0588	-0.9333	34°34'	38°26'	20.84	18.74	+200.74	+ 44.42
52- 6	-0.0565	-0.8378	23°41'	39°13'	30.40	18.38	+ 4.30	+241.94

Table IV. Constants of a damping sine curve obtained by solving the quadratic equation.

Curve No.	$\epsilon$	$n$	$T$	$A$	Curve No.	$\epsilon$	$n$	$T$	$A$
		° /	sec				° /	sec	
16-1	0.168	51 23	7.01	395.644	51- 1	0.197	41 06	17.56	642.659
16-2	0.049	49 01	7.34	273.748	51- 6	0.025	43 20	16.62	239.972
20-2	0.099	51 53	6.94	477.396	51-14	0.001	43 34	16.52	157.160
54-1	0.010	44 23	16.22	364.714	51-15	0.052	43 30	16.56	221.358
36-6	0.050	47 19	15.21	692.202	52- 1	0.138	39 27	18.26	711.766
37-2	0.063	36 33	19.70	204.716	52- 2	0.042	39 20	18.30	1051.983
37-3	0.079	44 03	16.34	213.050	52- 3	0.207	36 47	19.56	1530.230
37-4	0.083	48 29	14 86	226.346	52- 9	0.156	44 38	16.14	2578.848
37-5	0.262	43 14	16.66	197.462	52-10	0.280	42 47	16.84	280.259
37-6	0.102	48 23	14.88	154.754	52-12	0.077	44 24	16.28	258.741
37-7	0.196	45 14	15.92	133.194	52-13	0.01	43 49	16.44	232.288
49-1	0.181	42 11	17.03	360.774	52-15	0.005	39 27	18.26	1513.130
49-2	0.153	40 03	17.98	258.493	52-19	0.064	34 24	20.94	239.822
49-3	0.136	37 33	19.18	223.619	52-21	0.235	40 00	18.00	378.014
49-4	0.196	36 30	19.72	736.259	52-23	0.069	44 10	16.28	389.700
49-5	0.022	40 11	17.90	415.161	52-25	0.035	43 41	16.50	384.975
49-9	0.091	43 33	16.72	420.052					

Secondly, we picked up some curves of the simple form from Figs. 1~7, and calculated their periods and damping coefficients by solving a quadratic equation (24.7). The results are seen in Table IV and in Fig. 9. In the figure the values obtained by means of Takahasi's method are shown by small dots for comparison. As will be seen in Fig. 9 these calculated and observed values resemble each other closely.

These 32 oscillation curves here analysed are such fine sine curves that their periods are easily determined from their graphs by inspection. For comparison's sake the periods determined by inspection and by calculation are shown in the  $T'$  and  $T$  columns in Table V.

The difference between the two periods obtained by calculation and by inspection is extremely small, the probable error of their difference amounting to only  $\pm 0.3$  sec. For this reason, with all the rest of the curves not analysed by the method explained in § 24, we determined their periods by inspection.

Apropos of this, the errors of these theoretical curves will be shown in Table VI. From the observation equations given by (24.3), normal equations are formed. By solving the normal equations,  $s_i$  will be obtained, and when the values of  $s_i$  are replaced in (24.3), the residual  $v$  for each observation equation is given by

$$y_{\gamma} s_4 + y_{\gamma+1} s_3 + y_{\gamma+2} s_2 + y_{\gamma+3} s_1 + y_{\gamma+4} = v$$

From this  $v$  the probable error for each observation equation will be calculated. If we denote the probable error of  $y$  as  $r_y$  and put  $r_y = r / \sqrt{1 + \sum s_i^2}$  we shall be able to get some rough estimation of the errors. The  $r$  and  $r_y$  will be seen in Table VI-A. The values of  $r_y$  in Table VI-A are very small in comparison with the values of  $y$  in Table II, showing that the calculated results are fairly reliable. The values of  $r$  and  $r_y$  obtained by solving quadratic equations are given in column B of the same Table. The amount of errors they

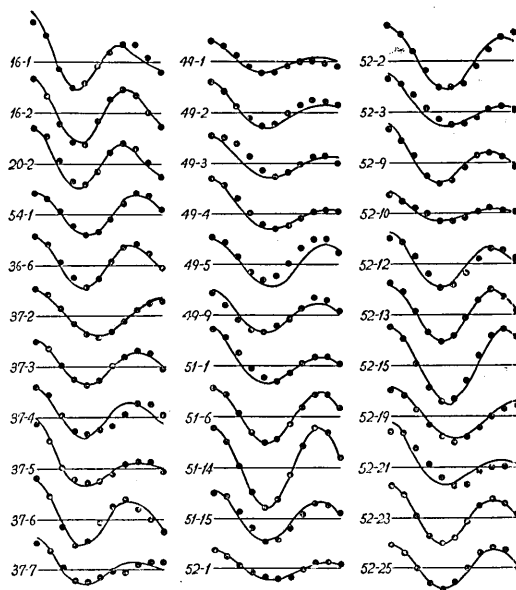


Fig. 9. · · ; Amplitudes obtained by means of the Takahasi-Husimi's method.  
· Full line ; Calculated curves obtained by solving the quadratic equation.

bring about in the calculated periods will be seen in the last column of the same table.

Table V. Comparison of  $T$  and  $T'$ .

$T$ ; Periods obtained from calculation.  
 $T'$ ; Periods obtained graphically,  $T' = \frac{1}{2}(Ta + 2Ti)$ .  
 $Ti$ ; Half periods of sine curves in Figs. 1~7.  
 $Ta$ ; One Periods of sine curves in Figs. 1~7.

Curve No.	$Ti$	$Ta$	$T'$	$T$	Curve No.	$Ti$	$Ta$	$T'$	$T$
36-5	8.6	16.4	16.8	16.80	51-11	8.4	16.8	16.8	16.22
36-6	7.4	15.4	15.1	15.21	51-14	8.4	16.6	16.7	16.52
37-2	9.8	19.4	19.5	19.70	51-15	8.4	16.6	16.7	16.56
37-3	8.2	16.6	16.5	16.34	52- 1	9.2	17.6	18.0	18.25
37-4	7.6	15.4	15.3	14.86	52- 2	9.2	18.8	18.6	18.30
37-5	8.4	16.8	16.8	16.70	52- 3	10.4	16.8	18.8	19.56
37-6	7.2	14.6	14.5	14.88	52- 9	8.4	16.2	16.5	16.14
49-1	8.8	16.8	17.2	17.08	52-10	8.6	16.4	16.8	16.80
49-2	8.8	17.2	17.4	17.98	52-12	8.4	16.4	16.6	16.28
49-3	9.6	17.8	18.5	19.18	52-13	8.4	16.2	16.5	16.44
49-4	10.2	18.8	19.6	19.72	52-15	8.8	18.4	18.0	18.26
49-5	9.0	17.4	17.7	17.92	52-18	9.6	19.2	19.2	19.06
49-9	8.4	16.8	16.8	16.72	52-19	10.4	20.2	20.5	20.94
51-1	9.0	17.2	17.6	17.56	52-21	9.6	18.6	18.9	18.00
51-6	8.2	16.6	16.5	16.62	52-23	8.2	16.4	16.4	16.28
51-9	8.8	17.6	17.6	17.84	52-25	8.2	16.4	16.4	16.50

Table VI. Errors of oscillation curves.

A			B			
Curve No.	$r$	$r_y$	Curve No.	$r$	$r_y$	$r_T$ sec.
19- 1	4.80	3.70	16- 1	8.93	5.24	1.60
20- 3	11.92	6.61	20- 2	8.38	5.18	1.21
54- 1	3.80	2.31	54- 1	3.20	1.58	1.49
34- 1	7.86	2.83	36- 6	3.35	2.50	1.72
36- 5	17.81	10.06	37- 2	3.07	1.50	2.84
37- 9	16.30	14.20	49- 1	4.67	2.69	3.02
49-10	11.71	9.00	51- 6	1.78	0.90	1.08
51-10	4.62	3.74	51-14	2.25	1.28	1.16
52- 4	18.95	12.55	52- 1	4.10	2.23	0.78
52- 6	22.38	12.01	52-23	3.11	1.21	1.62

## § 26. Periods of Oscillation Curves.

Now that oscillation periods have been calculated with regard to all the curves in Figs. 1-7, we shall proceed to the consideration of each of them.

The first three curves in Fig. 1 are those of the Sioyazaki earthquake. The next 19-1 is that of the Kesenuma earthquake (No. 19), composed of two curves of periods 6.4 sec. and 8.0 sec. respectively. The curves 20-1, 2, 3 belong to the Koti-Yamato earthquake (No. 20), and we obtain the periods of 6.8 sec. from 1 and 2, and 5.8 sec. and 18.5 sec. from 3. We obtain two periods of  $T_1=10.7$  sec. and  $T_2=16.4$  sec. from the curve 54-1 of the Kagi earthquake (No. 54), and two also from the Celebes Sea earthquake (No. 34),  $T_1=13.1$  sec. and  $T_2=19.8$  sec. With regard to the curves of the Celebes earthquake (No. 36), we obtain the period of about 20 sec. from the curves 35-1, 2, 3 analysed in the portion between 40 and 50 minutes, and the period of about 15 sec. from the curves 36-6~9 in the portion between 50 and 70 minutes. If we decompose 36-5 into two curves we have  $T_1=15.1$  sec.,  $T_2=21.7$  sec. In the Celebes earthquake two different periods seen to be present, namely  $T_1=15.4\pm 0.10$  sec. and  $T_2=20.3\pm 0.47$  sec. In the New Guinea earthquake (No. 37) we observe a period of 20 sec. at about 50 minutes and another of 15 sec. in the later portion, and in the still later portion, at about 70 min. from the *P* commencement, there are apparently two periods of about 16 sec. and 15 sec. Inclusive of tow periods appearing at about 50 minutes, we find three types of period in the New Guinea earthquake. The oscillation curves of the Mexico earthquake (No. 49) are shown in Fig. 4. A great majority of these curves have a period of 17 sec., but there exists the period of 20 sec. in 49-3, 4, and those of 16.4 sec. and 17.0 sec. in the neighbourhood of 100 minutes, that is, near the end portion. The oscillation curves of the Peru earthquake (No. 51) are seen in Fig. 5. Between 50 and 80 min. there exist two waves of 16.5 sec. and 19.5 sec., and in the later portions beyond 100 min., the waves with the period of 16.6 sec. are predominant. Figs. 6 and 7 are the results of the Chili earthquake (No. 52). In the portion of 50-80 min. there appear two periods of  $T_1=18.3$  sec. and  $T_2=20.2$  sec. Waves in this portion were named the first coda waves in Chapters 1-3, but then the mean periods in this part could not be decided accurately owing to the large fluctuation of the respective periods. Contrary to this, in the portion which we named the second coda, namely the part beyond 100 minutes, the mean values of the one-minute periods were fairly uniform according to the calculation performed in Chapters 1-3. With regard to this portion the period  $T_3=16.4$  sec. has been obtained both through the calculations performed and through Takahasi's method of analysis. All the periods obtained from the respective oscillation curves are shown in Table VII.

Table VII. Periods of oscillation curves.

Curve No.	<i>T</i>	Curve No.	<i>T</i>	Curve No.	<i>T</i>
	sec.		sec.		sec.
16-1	7.0	49- 1	17.1	52- 3	18.7, 19.6
16-2	7.3	49- 2	17.9	52- 4	20.8
16-3	7.1	49- 3	19.2	52- 5	18.0
19-1	6.4	49- 4	19.7	52- 6	18.2
20-1	6.8	49- 5	17.9	52- 7	16.3
20 2	6.9	49- 6	16.6	52- 8	16.6
20-3	5.9, 18.5	49- 7	17.3	52- 9	16.1
54-1	10.7, 16.4	49- 8	17.5	52-10	16.8
34-1	13.1, 19.8	49- 9	16.7	52-11	16.4
36-1	18.8	49-10	17.0, 16.4	52-12	16.3
36-2	21.7	51- 1	17.6	52-13	16.4
36-3	19.4	51- 2	17.8	52-14	16.3
36-4	15.9	51- 3	17.3	52-15	18.3
36-5	15.1, 21.7	51- 4	17.5	52-16	18.2
36-6	15.2	51- 5	17.4	52-17	18.3
36-7	15.6	51- 6	16.6	52-18	19.1
36-8	21.2	51- 7	19.8	52-19	20.9
36-9	15.3	51- 8	19.0	52-20	20.1
37-1	20.8	51- 9	17.8	52-21	18.0
37-2	19.7	51-10	17.8, 19.0	52-22	16.4
37-3	16.3	51-11	17.6	52-23	16.3
37-4	14.9	51-12	20.0	52-24	16.3
37-5	19.2, 16.7	51-13	17.4	52-25	16.5
37-6	19.7	51-14	16.5	52-26	16.2
37 7	15.9	51-15	16.6	52-27	16.4
37-8	15.6, 15.9	52- 1	18.3		
37-9	15.5	52- 2	18.3		

### § 27. Relations between the Epicentral Distance and the Coda Periods Revealed by Takahasi's Method.

If we divide the periods in Table VII into adequate groups with regard to each earthquake and make the mean of the respective groups, we are able to find the predominant periods of coda oscillations of the respective earthquakes, as are shown in Table VIII. From the table it appears that two or three sorts of waves of different periods are likely to exist in the coda oscillations of the respective earthquake. These are denoted by  $T_1$ ,  $T_2$  and  $T_3$ .

Table VIII. Predominant period determined by means of Takahasi-Husimi's method.

Earthq. No.	Epicerter	Comp.	Epicerter distance	$T_1$	$T_2$	$T_3$
16	Siwoya-Saki	E-W	295 km	7.1 <sup>sec</sup>	— sec	— sec
19	Kesenuma	N-S	380	6.4	—	—
20	Koti-Yamato	E-W & N-S	391	6.5	19.6	—
54	Kagi	N-S	2,230	10.7	—	16.4
34	Celebes Sea	E-W	4,110	13.1	19.8	—
36	Celebes	E-W	4,470	15.4	20.3	—
37	New Guinea	E-W	4,550	15.4	20.3	16.3
49	Mexico	E-W	11,600	17.3	19.5	16.6
51	Peru	E-W	14,900	17.5	—	16.6
"	"	N-S	"	17.6	19.5	16.6
52	Chili	E-W	16,800	18.3	20.2	16.4
"	"	N-S	"	18.2	20.0	16.4

and the relations between these periods and the epicentral distances of the respective earthquakes are shown in Fig. 10. From the table we notice at once that the  $T_1$  period agrees very well with the predominant period determined in the preceding chapters, and from the figure we see that as the epicentral distance increases  $T_1$  also increases. On the contrary, the  $T_2$  and

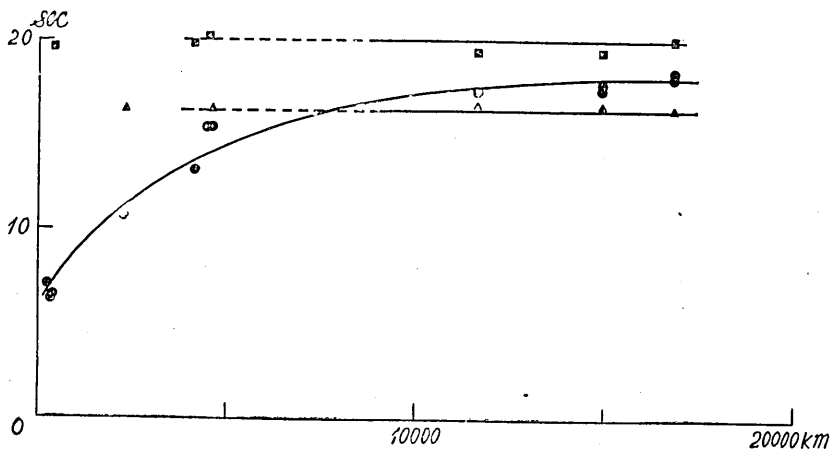


Fig. 10. Relations between predominant period determined from Takahasi-Husimi's method and epicentral distance.

●;  $T_1$ , ■;  $T_2$ , ▲;  $T_3$ .

$T_3$  apparently have the same values in all the earthquakes irrespective of the differences of their epicentral distances,  $T_2$  being roughly 20 sec. and  $T_3$  roughly 16 sec. In the predominant period obtained from the mean periods in the preceding chapters too, the period 16 sec. was found in the second coda waves of the earthquakes with the epicentral distances upwards of 10,000 km. Here, also, the period  $T_3$  was found mostly in the second coda waves of the earthquakes with long epicentral distances. It is also to be found in the first coda oscillations of New Guinea and Kagi earthquakes that have medium epicentral distances.

The  $T_2$  period has been observed in the first coda waves of the Mexico, Peru and Chili earthquakes, but as it existed mixed up with the oscillations of 17-18 sec. periods, its existence was not demonstrated until we had succeeded in separating these two periods by the method of analysis explained in the last paragraph. With respect to the earthquakes of Celebes, New Guinea and Celebes Sea too, the  $T_2$  period is seen to exist in the beginning part of the first coda oscillation.

Of these three types of periods that exist in the coda oscillations of earthquake motions,  $T_2$  and  $T_3$  have constant values in all the earthquakes without regard to their different epicentral distances. So it will not be unreasonable to assume that these represent the free oscillation periods of the vibrating system, while the  $T_1$  period that increases with epicentral distances is the period of external forces that reach the vibrating systems, namely, the period of the propagative seismic waves. However, the fact that we have adopted Takahasi's method of analysis presupposes that we are assuming the existence of some vibrating system. Therefore the question we have to consider is this:—What types of vibrating systems is it most proper for us to assume to exist?

As the free oscillation period of the seismometer used for recording earthquake motions has been kept up at about 60 sec., that observed period  $T_2$  can by no means be the free oscillation period of this seismometer. Another probable assumption is that the earth's surface layers upon which the seismometer is installed may constitute a vibrating system.

There have been repeated discussions regarding the possibility of occurrence of free vibrations in a surface layer, but if we assume its possibility in common with the prevailing opinions, we can find in it a convenient explanation for the three periods here observed.

During the period within which the sine type external waves stimulate the vibrating system, the system will continue forced oscillations and will display a  $T_1$  period, but as the periodicity of the external disturbance fades away and external forces come to have a nature of random stimulation to the vibrating

system, it will be expected that the free oscillation periods  $T_2$  and  $T_3$  will be observed. The study of the free oscillations of the surface layer will also afford an apt explanation to the phenomenon of  $T_1$  period appearing in one section of the first coda oscillations, and  $T_2$  in another, as in the case of the oscillatory curves here analysed.

In order that such a free oscillation might be maintained for a long time, the damping coefficient of the vibrating system will require some consideration. The damping coefficients of the respective waves of different periods are seen in Table IX. As seen in the table the dampings of the waves of free oscil-

Table IX. Damping constant  $h$  for respective oscillation curves.

Curve No.	$T_1$	$h$	Curve No.	$T_2$	$h$	Curve No.	$T_3$	$h$
	sec			sec			sec	
16- 1	7.0	0.0866	34- 1	19.8	0.1212	54- 1	16.4	0.0119
16- 2	7.3	0.0439	36- 1	18.8	0.1676	37- 3	16.3	0.0814
19- 1	6.4	0.3358	36- 5	21.7	0.0556	37- 5	16.7	0.2690
20- 2	6.9	0.0778	37- 2	19.7	0.0848	37- 9	15.9	0.0930
54- 1	10.7	0.2673	37- 7	20.0	0.2273	49- 9	16.6	0.0960
34- 1	13.1	0.5573	49- 3	19.5	0.1741	49-10	16.4	0.0156
36- 6	15.2	0.0461	49- 4	19.7	0.2565	51- 6	16.6	0.0272
37- 4	14.9	0.0734	51-10	19.0	0.5511	51-14	16.5	0.0002
37- 6	14.9	0.0907	52- 3	19.6	0.2674	51-15	16.6	0.0552
37- 9	15.5	0.3501	52-18	19.7	0.0992			
49- 1	17.1	0.1959	52-19	20.9	0.0936			
49- 2	17.9	0.1790						
49- 5	17.9	0.0402						
49-10	17.0	0.3337						
51- 1	17.6	0.2211						
51- 3	17.3	0.0538						
51- 4	17.5	0.0943						
51- 9	17.8							
51-10	17.8	0.0406						
52- 1	18.3	0.0522						
52- 2	18.3	0.0522						
52- 4	18.7	0.0850						
52- 6	18.2	0.7161						
52-15	18.3	0.0066						
52-21	18.0	0.2704						

lation are smaller than those of the waves that propagate, and the waves of  $T_3$  period display particularly small damping coefficients.

As to the free oscillation in the surface layer, E. Wiechert<sup>4)</sup> advanced the theory of a stationary wave that has a node at the lower end of the surface layer and a loop at the surface of the layer. If we take up such a model, the thickness of the layer  $d$  will be represented by  $d = \frac{1}{2} VT$ , where  $V$  is the velocity of the elastic shear waves that pass through the layer, and  $T$  the period of the stationary waves. Now if we give to  $d$  and  $V$  in the upper and middle layers the values  $d_1 = 4.5$  km,  $d_2 = 16$  km,  $V_1 = 1.1$  km/sec and  $V_2 = 3.2$  km/sec respectively, according to the result of T. Matuzawa,<sup>5)</sup> we shall be able to expect the periods of the stationary waves to be  $T_3 = 16$  sec., and  $T_2 = 20$  sec. These, however, are quite rough estimations, and we will discuss them in detail in the following chapters.

In concluding this chapter the author wishes to express his cordial thanks to Professors T. Hagiwara and Ch. Tsuboi for their kind advices and continuous encouragement throughout the course of this study.

## 20. 地震動の尾部について (其の 5)

地震研究所 表俊一郎

第 6 章 高橋伏見の方法による地震動の尾部の週期解析.

高橋伏見の方法により震央距離の異なる 9 個の地震について尾部の振動の週期解析を行つた結果をのべた。まず始めに高橋伏見の方法により解析を行へば得られる振動曲線は 2 つの減衰性正弦波が重ね合せられたものとなることをのべ次に之を夫々の component curve に分解して夫々の曲線の減衰率と週期とを求める方法を述べた。このようにして 53 個の振動曲線より 70 本の正弦曲線を求め尾部の週期を解析した所、前章迄では正確な週期を見出すことの出来なかつた第 1 尾部の部分についても充分正確に解析を進めることが出来地震動の尾部には 3 つの種類の週期の群が見られることが明らかになつた。之等を  $T_1$ ,  $T_2$  及び  $T_3$  と名付けた。 $T_1$  は震央距離の大きい地震程大きな値を示す週期であり  $T_2$  及び  $T_3$  は之に反して震央距離の如何に拘はらず常に一定の値を示すものであり  $T_2$  は主として第 1 尾部、 $T_3$  は第 2 尾部の振動の中に見られその値は略々  $T_2 = 20$  秒  $T_3 = 16$  秒となることを知る事が出来た。

4) E. WIECHERT und K. ZÖPRITZ, "Über Erdbeben Wellen" Göttingen, 1907, 54.

5) T. MATUZAWA, *Bull. Earthq. Res. Inst.*, 6 (1929), 177.